

# CONTAINERLESS SOLIDIFICATION STUDIES OF THE 1/1 PHASE IN TI-(MN,CR,FE)-SI-O ALLOYS

T.K.Croat \*, K.F. Kelton \*, D. Holland-Moritz \*\*, T.J. Rathz \*\*\*, M.B. Robinson \*\*\*\*

\* Physics Department, Washington University, St. Louis, MO 63130,

\*\* Institut für Raumsimulation, DLR, D-51170, Köln, Germany

\*\*\* University of Alabama, Huntsville, AL

\*\*\*\* NASA/ George C. Marshall Space Flight Center, Huntsville, AL 35812

## ABSTRACT

The nucleation behavior of the 1/1 quasicrystal approximant phase was investigated in Ti-TM-Si-O (TM=Mn, Cr, Fe) alloys made near the stoichiometric composition. Containerless solidification studies were performed using electromagnetic (rf) levitation and drop-tube techniques. The solidification microstructures indicate that  $\alpha$ -Ti nucleated first in Ti-Cr-Si-O and  $\beta$ -Ti in Ti-Mn-Si-O alloys; the 1/1 phase nucleated and grew on these titanium oxide dendrites. In Ti-Fe-Si-O alloys, the 1/1 phase nucleated and grew directly from the liquid, allowing information on the nucleation rates to be obtained from undercooling data.

## INTRODUCTION

The microstructures of Ti-TM-Si-O alloys made near the icosahedral phase (i-phase) or crystal approximant ( $\alpha$ -1/1) compositions are sensitive to the concentrations of oxygen and silicon. Rapidly solidified alloys made near the  $\alpha$ -1/1 composition contain a dense dispersion of 150-250 nm grains, primarily of the 1/1 phase. The proposed similarities between the local atomic structures of the i-phase, the 1/1 approximant and the liquid, suggest that the nucleation rate of  $\alpha$ -1/1 should be higher than for simpler crystals, explaining the high grain density. As the composition is shifted from that of the 1/1 phase, the grain density decreases.<sup>1</sup> This signals a decrease in the nucleation rate possibly arising from an increased interfacial free energy as the composition of the liquid is shifted away from that of  $\alpha$ -1/1. To investigate this further, solidification studies were performed using drop-tube and rf-levitation techniques. A central goal was to identify alloys where the  $\alpha$ -1/1 phase was the primary solidification product, nucleating directly from the liquid. Our studies demonstrate that for low cooling rates,  $\alpha$ -Ti and  $\beta$ -Ti are the primary solidification phases in the Ti-Cr-Si-O and the Ti-Mn-Si-O alloys, respectively. The stoichiometric Ti-Fe-Si-O  $\alpha$ -1/1, requiring less oxygen, is the primary solidification product. Our initial results show lower relative undercoolings in alloys forming  $\alpha$ -1/1 primarily, suggesting a higher nucleation rate than competing crystal phases.

## EXPERIMENT

Alloy components (Ti 99.97%, Cr 99.99%, Fe 99.98%, Mn 99.9%, Si 99.999%, SiO<sub>2</sub> 99.99%, TiO 99.9%) were mixed in the correct proportions and arc-melted repeatedly in Ar gas to produce homogeneous ingots. Oxygen was incorporated into the as-cast ingots by the addition of either TiO or SiO<sub>2</sub>. Chemical analysis and microprobe measurements on as-cast ingots show average oxygen concentrations that are in good agreement with those expected from the starting components for both methods.<sup>1</sup> For the rf-levitation and drop tube solidification studies, approximately spherical arc-melted samples of typically 6-7 mm diameter were used. As-cast samples, in contact with a water-cooled copper hearth, are cooled from the liquid at rates of  $\approx 100^\circ\text{K}/\text{sec}$ . For rf-levitation studies, samples were inductively heated above their liquidus temperatures, and subsequently cooled at tens of degrees per second using a helium gas jet. Heating and undercooling cycles were applied multiple times to ensure repeatability. Further

experimental details are given elsewhere.<sup>1</sup> Drop tube solidification experiments were performed in the 105m tube at Marshall Space Flight Center in Huntsville, AL.<sup>2</sup> As-cast ingots were melted and subsequently cooled at hundreds of degrees per second during free fall through He gas. Microstructure and phase information were obtained by powder x-ray diffraction (XRD) using  $\text{CuK}\alpha$  radiation, scanning electron microscopy (SEM), using a Hitachi S-4500 SEM equipped with a backscattered electron detector, and transmission electron microscopy (TEM) using a JEOL 2000-FX TEM. Phase composition was determined in SEM and TEM by energy dispersive x-ray spectroscopy (EDS).

## RESULTS AND DISCUSSION

The phase formation is particularly sensitive to the oxygen concentration. EDS measurements in TEM on individual  $\alpha$ -1/1 grains reveal the stoichiometric composition to be  $\text{Ti}_{68}\text{Fe}_{26}\text{Si}_6$ ,  $\text{Ti}_{60}\text{Cr}_{30}\text{Si}_{10}$ , and  $\text{Ti}_{60}\text{Mn}_{37}\text{Si}_3$ .<sup>1</sup> Although a distinct oxygen peak is detectable in EDS, an accurate measurement of this low energy peak is not possible and, further, surface oxygen contributes strongly to the signal. Based on XRD, oxygen incorporation is necessary to maximize the volume fraction of the  $\alpha$ -1/1 phase. Up to 20 at.% oxygen is required in Ti-Cr-Si-O alloys, whereas Ti-Mn-Si-O alloys require 6 at. % oxygen and Ti-Fe-Si-O alloys require only 4 at %.<sup>1</sup> Annealing experiments demonstrate that oxygen thermodynamically stabilizes the approximant phases, presumably due to a stabilization of local icosahedral coordination in the liquid.<sup>3</sup> To investigate this further, solidification studies were performed on samples prepared with variable oxygen concentrations.

### As cast Solidification Studies

As a necessary precursor to the containerless solidification experiments, the composition range over which the  $\alpha$ -1/1 formed was investigated. Studies of as-cast ingots were made in Ti-TM-Si-O (TM={Cr, Mn, Fe }) alloys prepared near the previously determined approximant phase stoichiometries. X-ray diffraction patterns from as-cast ingots made at the 1/1 phase stoichiometry for each of these three alloy systems are shown in fig. 1. These patterns show predominate formation of the 1/1 approximant phase, along with other minority phases. The minority phases present are listed in table I. Based on XRD, the 1/1 phase constitutes 85%, 80%, and 60% by volume fraction for Ti-Fe-Si-O, Ti-Cr-Si-O, and Ti-Mn-Si-O, respectively.

Microstructural analysis was made with SEM to determine the phase formation sequence in these alloys. Suitable thinning of large regions for TEM observation proved difficult in these brittle materials, so extensive examination of powdered samples by TEM diffraction was used to identify the phases present. The identified phases were correlated with microstructural features in SEM using EDS on both microscopes. It should be noted that oxygen concentrations quoted are based on the starting compositions. Typical composition and crystallographic information for all phases identified are listed in table I.

SEM studies of Ti-Cr-Si-O as-cast alloys prepared near the stoichiometric composition (with oxygen at 10-20 at. %) showed that  $\alpha$ -Ti nucleates first (not the  $\alpha$ -1/1 phase) and grows dendritically from the liquid (Fig. 2a). Surrounding the dendrites are approximately spherical grains of  $\alpha$ -1/1 with a typical diameter of 20-30  $\mu\text{m}$ , growing in a peritectic fashion. The low solubility of  $\alpha$ -Ti for 3d transition metals causes a Cr enrichment of the liquid, leading to the formation the  $\text{TiCr}_2$  phase as the final solidification product at the  $\alpha$ -1/1 grain boundaries.

Due to the high oxygen concentration of the alloy, primary formation of  $\alpha$ -Ti is not surprising. Oxygen stabilizes the structure of  $\alpha$ -Ti; its liquidus temperature rises from 1250°K to 2100°K as oxygen is increased from 5 to 20 at.%. Attempts to reduce the stability of this phase by decreasing oxygen resulted instead in the primary solidification of the C14  $\text{TiCr}_2$  Laves phase.

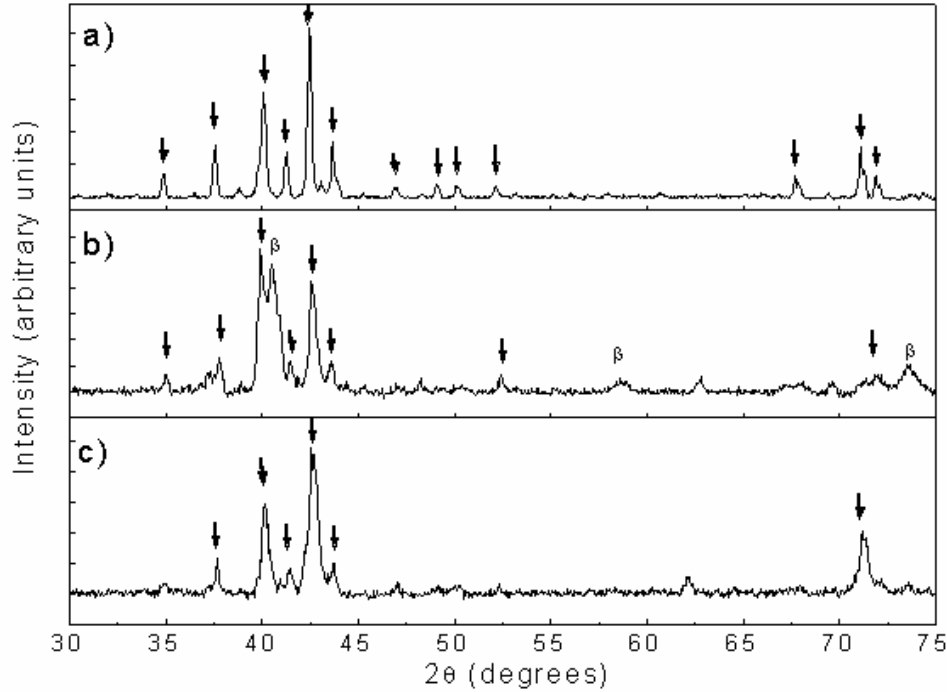


Fig. 1. XRD scans of a)  $\text{Ti}_{60}\text{Cr}_{30}(\text{SiO}_2)_{10}$  b)  $\text{Ti}_{60}\text{Mn}_{37}(\text{SiO}_2)_3$  and c)  $\text{Ti}_{68}\text{Fe}_{26}\text{Si}_4(\text{SiO}_2)_2$ . Arrows indicate the positions of 1/1 approximant peaks of the  $\alpha$ -1/1.

Table I. Phases found in Ti-{Cr,Mn,Fe}-Si-O alloys

Alloy	Phase	Crystallography	Composition
Ti-Cr-Si-O	1/1 approximant	bcc type: $a = 13.0\text{\AA}$	$\text{Ti}_{60}\text{Cr}_{30}\text{Si}_{10}$
	C14 $\text{TiCr}_2$ Laves	hexagonal: $a = 4.9\text{\AA}$ , $c = 8.0\text{\AA}$	$\text{Ti}_{38}\text{Cr}_{58}\text{Si}_4$
	$\alpha$ -Ti	hcp: $a = 3.0\text{\AA}$ , $c = 4.8\text{\AA}$	$\text{Ti}_{95}\text{Cr}_4\text{Si}_1$
Ti-Mn-Si-O	1/1 approximant	bcc type: $a = 13.0\text{\AA}$	$\text{Ti}_{60}\text{Mn}_{37}\text{Si}_3$
	$\beta$ -Ti	bcc: $a = 3.0\text{\AA}$	$\text{Ti}_{72}\text{Mn}_{25}\text{Si}_3$
	C14 $\text{TiMn}_2$ Laves	hexagonal: $a = 4.9\text{\AA}$ , $c = 8.0\text{\AA}$	$\text{Ti}_{36}\text{Mn}_{60}\text{Si}_4$
	$\lambda$ decagonal approximant	orthorhombic: $a = 32.1\text{\AA}$ $b = 26.2\text{\AA}$ $c = 15.7\text{\AA}$	$\text{Ti}_{58}\text{Mn}_{40}\text{Si}_2$
Ti-Fe-Si-O	1/1 approximant	bcc: $a = 13.1\text{\AA}$	$\text{Ti}_{68}\text{Fe}_{26}\text{Si}_6$
	TiFe	CsCl-type $a = 3.0\text{\AA}$	$\text{Ti}_{58}\text{Fe}_{38}\text{Si}_4$
	$\text{Ti}_2\text{Fe}$	fcc: $a = 11.3\text{\AA}$	$\text{Ti}_{64}\text{Fe}_{31}\text{Si}_5$

In samples prepared with 5 at.% oxygen, the  $\text{TiCr}_2$  Laves phase nucleates and grows dendritically from the liquid, followed by the formation of the 1/1 phase. In samples prepared with no oxygen, the Laves and  $\beta$ -Ti phases form simultaneously with a lamellar eutectic microstructure.

Similar problems with the primary nucleation of  $\alpha$ -1/1 were encountered in Ti-Mn-Si-O alloys, where  $\alpha$ -1/1 formed competitively with  $\beta$ -Ti, the  $\text{TiMn}_2$  Laves phase, and the  $\lambda$  phase.  $\beta$ -Ti crystallized dendritically at the stoichiometric composition of  $\text{Ti}_{60}\text{Mn}_{37}(\text{SiO}_2)_3$  (Fig. 2b). The  $\alpha$ -

1/1 and  $\lambda$  phases then solidified followed by trace amounts of the Laves phase. As-cast samples prepared without oxygen formed a mixture of  $\beta$ ,  $\lambda$ , and the Laves phase. Again, no 1/1 phase was found in the oxygen-free samples.

In Ti-Fe-Si-O alloys, a narrow compositional window was found in which  $\alpha$ -1/1 was the primary phase. Near 4 at %,  $\alpha$ -1/1 formed as approximately spherical 5  $\mu\text{m}$  grains, surrounded by the TiFe phase (Fig. 2c). With lower oxygen concentrations, the 1/1 phase was again supplanted by the TiFe<sub>2</sub> Laves and  $\beta$  phases. At higher oxygen concentrations (8 at.%),  $\alpha$ -Ti dendrites grew from the liquid.

#### Drop Tube Solidification Studies

Attempts were made to solidify directly to  $\alpha$ -1/1 in Ti-Cr-Si-O and Ti-Mn-Si-O alloys using the more rapid containerless cooling accessible in the 105 m NASA Drop-Tube at Marshall Space Flight Center. Alloys of Ti-Cr-Si-O were prepared near the stoichiometry of the  $\alpha$ -1/1, with 0, 15 and 20 at. % oxygen. No qualitative difference between drop tube processed and as-cast samples was observed for the 15 and 20 at.% oxygen samples. Again, dendrites of  $\alpha$ -Ti grew from the liquid. Roughly spherical grains of  $\alpha$ -1/1 grew in a peritectic manner from the liquid on these dendrites, and the C14 TiCr<sub>2</sub> Laves phase solidified last. Samples made without oxygen showed no evidence of the 1/1 phase. Instead  $\beta$ -Ti and the C14 Laves phase grew with an anomalous eutectic microstructure, where the lamella observed in as-cast samples developed into multiple domains due to the high undercooling. In some regions, the Laves appeared to be growing dendritically from the liquid.

The microstructures of Ti-Mn-Si-O alloys processed in the drop-tube showed competitive formation of  $\alpha$ -1/1 and the  $\lambda$  phase. At the stoichiometric composition of Ti<sub>60</sub>Mn<sub>37</sub>(SiO<sub>2</sub>)<sub>3</sub>, a Ti-rich phase with composition Ti<sub>80</sub>Mn<sub>19</sub>Si<sub>1</sub>, most likely  $\beta$ -Ti, crystallized dendritically. The interdendritic liquid then solidified to the  $\alpha$ -1/1 and  $\lambda$  phases. Primary 1/1 formation was not achieved. In both Ti-Mn-Si-O and Ti-Cr-Si-O, a minor volume fraction crystallized primarily and released undetectable recalescences, which prevented measurements of the achieved undercooling levels.

#### Electromagnetic Levitation Studies

Rf-levitation studies allowed direct monitoring of the maximum undercooling of the alloys, allowing limits to be placed on the homogeneous nucleation rate. Although cooling rates were not as rapid, the quiescent environment gave repeatable undercooling data.

Preliminary studies of levitated Ti-Fe-Si-O alloys indicated an ability to observe the nucleation of the 1/1 phase from the liquid. The undercooling behavior was studied as a function of composition by fixing the O and Si, while varying the concentrations of Ti and Fe, which allowed finer compositional control. As for the as-cast samples, the microstructure of alloys prepared at the  $\alpha$ -1/1 stoichiometry contained approximately spherical grains of  $\alpha$ -1/1 (average diameter of 5  $\mu\text{m}$ ) surrounded by the TiFe phase (Fig. 3a). The convex shape of the 1/1 grains is evidence that these formed directly from the liquid. A similar morphology for  $\alpha$ -1/1 was observed in Ti<sub>x</sub>Fe<sub>94-x</sub>Si<sub>4</sub>(SiO<sub>2</sub>)<sub>2</sub> alloys with 67 < x < 70. Lower magnification examinations show no evidence of any dendritic microstructure (Fig. 3b). Over the same composition range, the 1/1 phase is the primary phase in the as-cast samples as well. Alloys made with less Ti showed primary dendritic growth of an unidentified phase, followed by faceted growth of Ti<sub>2</sub>Fe on the dendrites (Fig. 3c). Alloys made with a higher Ti concentration show less well-formed dendrites of composition Ti<sub>74</sub>Fe<sub>19</sub>Si<sub>7</sub>, most likely  $\beta$ -Ti (Fig. 3d).

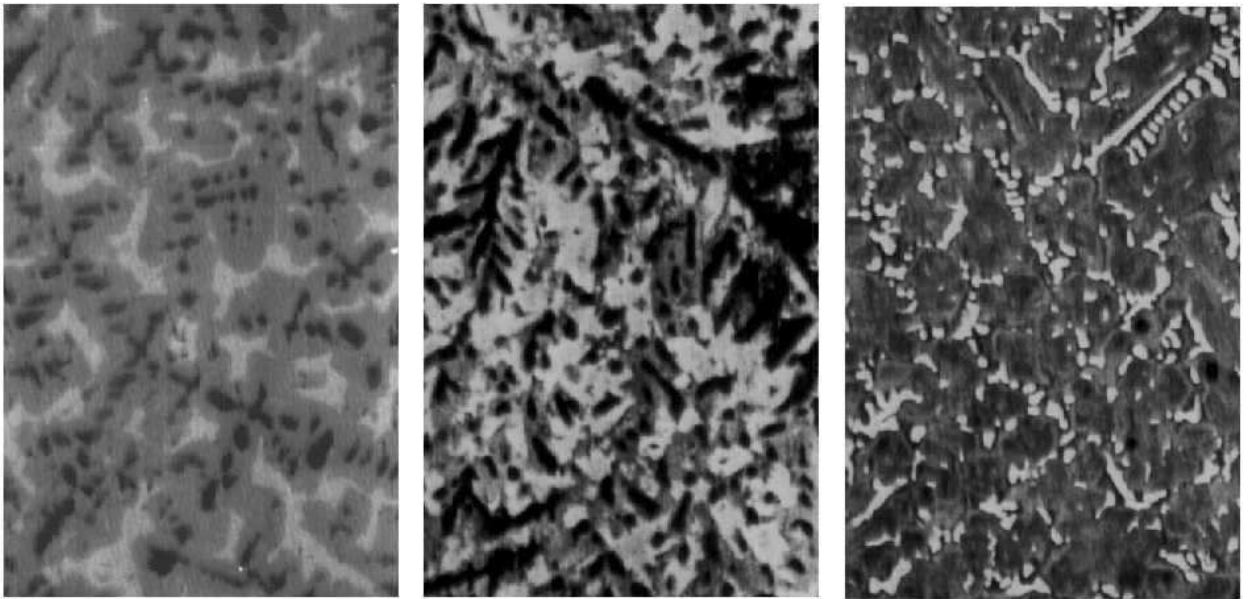


Fig. 2 As cast microstructure of stoichiometric 1/1 phase in  
 a) Ti-Cr-Si-O b) Ti-Mn-Si-O and c) Ti-Fe-Si-O

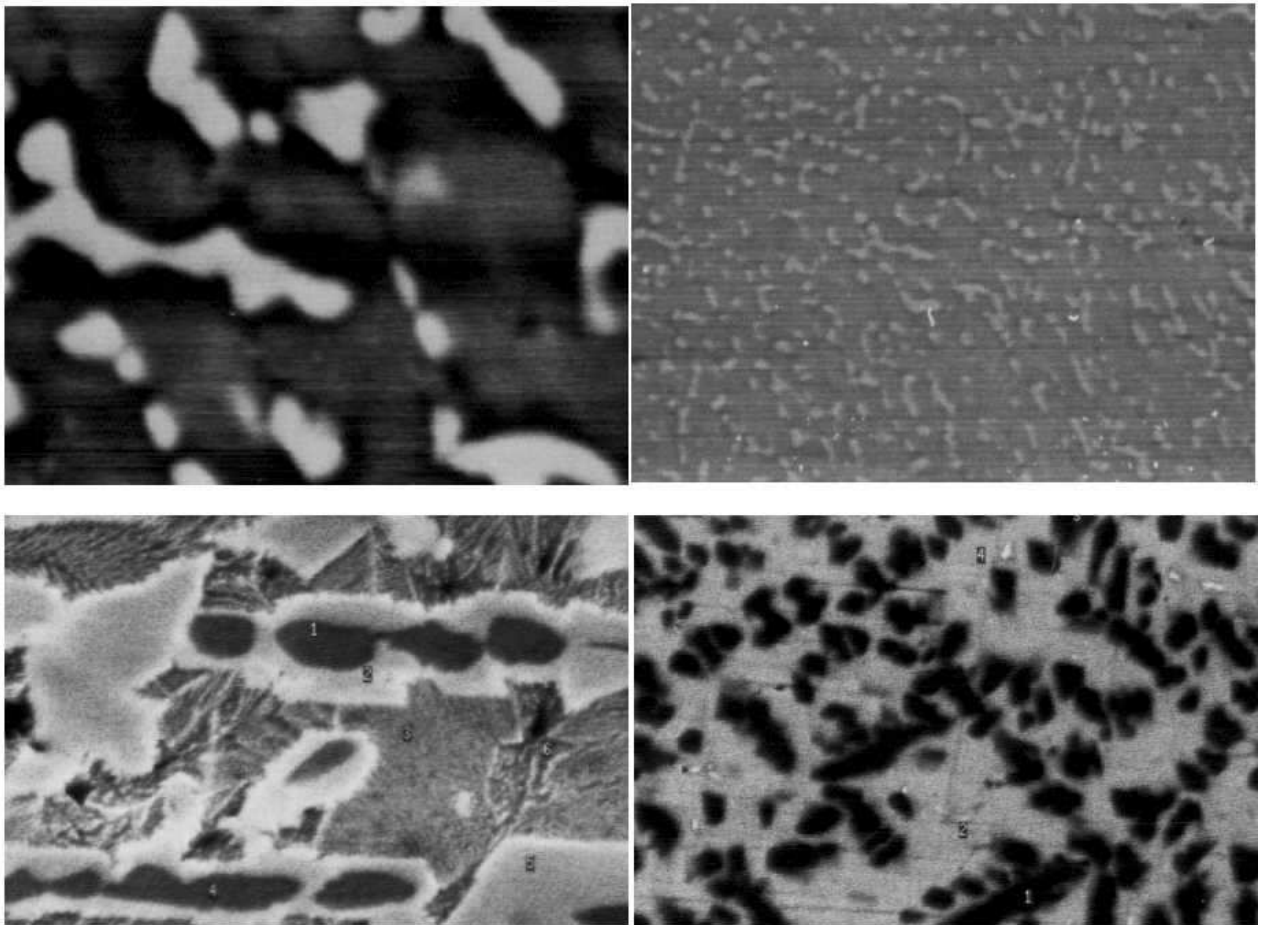


Fig. 3. Back-scattered SEM images of electromagnetically levitated samples in Ti-Fe-Si-O.  
 a)  $\text{Ti}_{67}\text{Fe}_{27}\text{Si}_4(\text{SiO}_2)_2$  b)  $\text{Ti}_{68}\text{Fe}_{26}\text{Si}_4(\text{SiO}_2)_2$  c)  $\text{Ti}_{66}\text{Fe}_{28}\text{Si}_4(\text{SiO}_2)_2$  and d)  $\text{Ti}_{71}\text{Fe}_{23}\text{Si}_4(\text{SiO}_2)_2$

Alloys prepared at the  $\alpha$ -1/1 stoichiometry had lower relative undercoolings ( $\Delta T/T_{\text{melt}} \approx 0.1$ ) than other crystal phases found at higher Ti compositions ( $\Delta T/T_{\text{melt}} \approx 0.18$ ) (Fig. 5). This presumably reflects a higher nucleation rate of the  $\alpha$ -1/1 due to the strong similarity in local atomic structures between the approximant and the liquid. Changes in the post-recalcescence temperature also reflect the difference in the solidification behavior. Near the stoichiometric composition, the temperature rise was negligible after the onset of solidification, consistent with a small undercooling and slow growth. On either side of this composition, the post-recalcescence temperature rise was substantially larger, suggesting a greater undercooling below the liquidus of the primary solidifying phase.

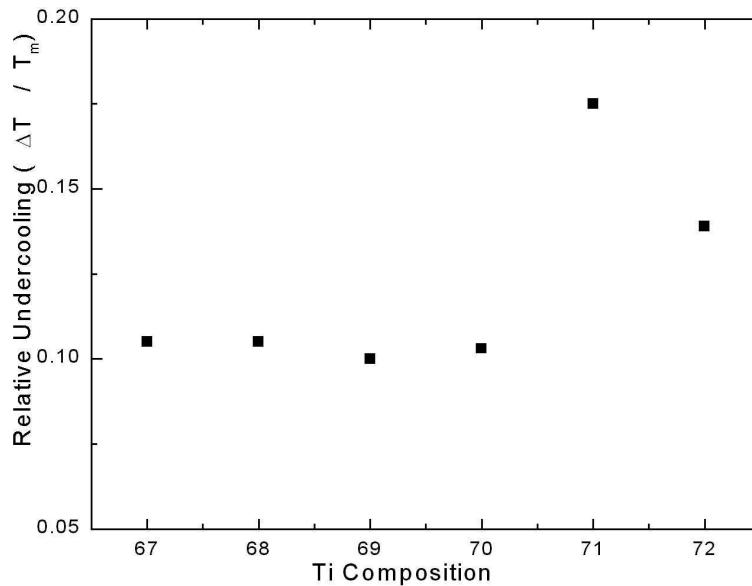


Fig. 4. Maximum Relative Undercooling vs. Composition in Ti-Fe-Si-O

## CONCLUSIONS

The solidification microstructure and formation of the approximant phase from the alloy melt in titanium-based quasicrystal forming alloys was studied. In Ti-Cr-Si-O and Ti-Mn-Si-O alloys, the high melting  $\alpha$ -Ti and  $\beta$ -Ti phases formed primarily, inhibiting studies of the nucleation of the icosahedrally-coordinated phases. In Ti-Fe-Si-O alloys, however, primary solidification of the 1/1 phase were observed. Preliminary studies show lower relative undercoolings near the stoichiometry of the 1/1 phase, indicating a greater structural similarity of this phase and the liquid than for the other crystalline phases.

## ACKNOWLEDGMENTS

Partially supported by NASA under contract NAG 5-908 and NGT 5-50030, and by Deutsche Forschungsgemeinschaft (DLR-BO). Additional thanks to Thomas Schenk and Dieter Herlach for their help and useful discussions.

## REFERENCES

1. J.L. Libbert and K.F. Kelton, *Phil. Mag. Lett.*, **71**, 213 (1995).
2. D. Holland-Moritz, D.M. Herlach, and K. Urban, *Acta Met.* **46** (5), 1601 (1998).
3. T.J. Rathz, M.B. Robinson, W.H. Hofmeister, and R.J. Bayuzick, *Rev. Sci. Instrum.* **61**, 3846 (1990).
4. J.L. Libbert, J.Y. Kim, and K.F. Kelton, *Phil. Mag. A*, **79**, 2209 (1999).